

---

# Influence of Temperature and Time on $\text{Nd}_2\text{O}_3\text{-SiO}_2$ Composite Prepared by the Solgel Process

S. DUHAN<sup>a</sup> AND P. AGHAMKAR<sup>a,b,\*</sup>

<sup>a</sup>Materials Science Lab, Department of Applied Physics  
Guru Jambheshwar University of Science and Technology  
Hisar-125001, India

<sup>b</sup>Department of Physics, Chaudhary Devi Lal University  
Sirsa-125055, India

*(Received December 5, 2007; in final form February 22, 2008)*

Using solgel method  $\text{Nd}_2\text{O}_3\text{-SiO}_2$  binary oxide systems were prepared. The binary oxide transformed from the amorphous phase to nanocrystalline phase upon heat treatment in air. Characterization of the  $\text{Nd}_2\text{O}_3\text{-SiO}_2$  was carried out by using X-ray diffraction, Fourier transform infrared spectroscopy, and scanning electron microscopy. The effect of the sintering temperature and time on the evolution of the binary oxide system was discussed. It is found that sintering time plays a pivotal role to obtain  $\text{Nd}_2\text{O}_3\text{-SiO}_2$  nanocomposite. At temperature of  $900^\circ\text{C}$ , the sample was sintered for 12 h and monoclinic  $\text{Nd}_2\text{O}_3$  nanocrystallites, with average crystallite size  $\approx 12$  nm, were obtained.

PACS numbers: 61.46.Df, 61.46.Hk, 78.67.Bf

## 1. Introduction

Nanocrystalline materials with tailored structure and properties are expected to have a great technological importance. Over the past few years, there has been considerable interest in the study of binary oxide systems containing nanocrystalline  $\text{Ln}_2\text{O}_3$  (Ln, lanthanide) and silica due to their importance in many fields of technology, to name a few, photonics, microelectronics, sensors and catalysts, etc. [1, 2]. Applications of the nanomaterials are very interesting specially in the field of photonics and catalysis because of a quantum size phenomenon. This

---

\*corresponding author; e-mail: prasut2003@yahoo.co.in and surender6561@yahoo.co.in

phenomenon significantly affects characteristics and performance of the photonics and catalysts, e.g. enhancement of emission lifetime, luminescence, quantum efficiency, optical nonlinearity and chemical activity (dehydrogenation/hydrogenation and esterification etc.) [3–6].

Recently, a large variety of techniques have been turned out for preparing of composites at the nanometer scale. Among lanthanides,  $\text{Nd}_2\text{O}_3$  has been widely used in photonic applications [7], luminescence [8], catalyst or catalyst promoters [9–12] and protective coatings etc. [13, 14]. For the most of these applications the ultrafine (in nanometer scale) neodymium oxides with well defined particle morphology are the most essential materials. Therefore, preparation and characterization of  $\text{Nd}_2\text{O}_3$  nanoparticles have attracted much attention in recent years. Recently,  $\text{Nd}_2\text{O}_3$  nanocrystalline has been synthesized by the inverse micro-emulsion technique, direct precipitation from high boiling polyalcohol solutions, solvothermal and hydrothermal reaction routes [8, 15, 16]. In the present article, solgel technique is being used for the preparation of  $\text{Nd}_2\text{O}_3$  nanocrystallites in a silica matrix. Silica has been used as a host matrix due to its high softening temperatures, high thermal shock resistance, and low index of refraction [17–19].

The solgel processes combine the advantage of lower temperature and possibility of making of finely dispersed powders, films, fibers and coating [20]. Rare-earth oxides, due to their special properties, have also been used in many fields such as ceramic industry and sensors. As we know, the smaller the particles size, the larger the specific surface area, and the higher the activity. Thus synthesis of different structure/phases of Ln oxides nanocrystallites, is in great demand to fulfill the requirements of technology and industry. The development of new binary (rare-earth oxides and silica) systems and their characterization are important not only for technological reasons but also for obtaining a better understanding. Literature survey [12, 21, 22] reveals that formation of rare-earth oxides/silicates inside or at the surface of amorphous  $\text{SiO}_2$  matrix depends on the synthesis method, rare-earth oxide and silica molar ratio and thermal/pressure treatment.

In the present report, the effect of sintering temperature and time on the evolution of the  $\text{Nd}_2\text{O}_3$ - $\text{SiO}_2$  has been investigated and found that the thermal treatment at temperature of  $900^\circ\text{C}$  with prolonged sintering (12 h) develops the monoclinic  $\text{Nd}_2\text{O}_3$  phase with well defined particle morphology. The  $\text{Nd}_2\text{O}_3$ - $\text{SiO}_2$  binary oxide system is characterized by X-ray diffraction (XRD), Fourier transform infrared spectroscopy (FTIR), and scanning electron microscopy (SEM). The average size of neodymium oxide nanocrystallites in a fused silica matrix was found to be  $\approx 12$  nm.

## 2. Experimental

### 2.1, Sample preparation

Neodymia-silica (binary oxide) composites were prepared by the solgel method. The high purity reagents: tetraethoxy silane (Aldrich 99.999), ethanol

(Aldrich 99.9995), and deionized water were mixed in the presence of hydrochloric acid as catalyst (Aldrich 99.995). 6 wt% neodymium oxide was introduced in the pre-hydrolyzed solution in the form of nitrate under heating. The hygroscopic nature of the  $\text{Nd}(\text{NO})_3$  salt does not allow its exact weighing, thus the salt was dissolved in deionized water and metal content was determined by standard titration. The pH of the resultant solutions was 3.5. The solutions were filled in quartz ( $10 \times 20 \times 45 \text{ mm}^3$ ) and kept in a drying oven (GFL-7105) at  $120^\circ\text{C}$ . It was observed that the gelation acts after approximately 3 days. Even after the gelation, the samples were still kept inside the oven for few days for aging. The aging process allows further shrinkage and stiffening of the gel. The color of the doped samples was glassy violet-purple due to the presence of neodymia. The powder form of the doped samples was obtained by pestle and mortar. The powder samples were sintered in muffle furnace (KSL 1600X, MTI) in air.

### 2.2. Characterization

Complementary methods were used to characterize the structure of the doped samples. X-ray diffraction pattern of samples were carried out by a Philips X-ray diffractometer PW/1710; with Ni filter, using monochromatic  $\text{Cu } K_\alpha$  radiation of wavelength  $1.5418 \text{ \AA}$  at 50 kV and 40 mA. SEM of the samples was done with JEOL-JSM-T330-A 35 CF microscope at an accelerating voltage of 20 kV. Infrared spectra were collected with a Perkin Elmer 1600 (spectrophotometer) in  $1250\text{--}500 \text{ cm}^{-1}$  range.

## 3. Results and discussion

### 3.1. XRD

X-ray diffraction patterns of sintered binary oxides ( $\text{Nd}_2\text{O}_3\text{--SiO}_2$ ) are shown in Fig. 1. The powdered sample sintered at  $600^\circ\text{C}$  (6 h) shows no strong and sharp diffraction peak, which infers that the powder is still amorphous. This result suggests that heating of binary oxides at low temperature for six hours is not effective for achieving initial crystallization phase of the  $\text{Nd}_2\text{O}_3\text{--SiO}_2$ . In order to achieve crystallinity, the sintering temperature was increased up to  $900^\circ\text{C}$  and the sample was sintered for 12 h. In this condition a significant change in the diffraction patterns was observed. The two major strong diffraction peaks appeared around  $2\theta \approx 27.5^\circ$  and  $29.2^\circ$ . These peaks may be assigned to (010) and ( $\bar{4}$ 02) of monoclinic  $\text{Nd}_2\text{O}_3$  phase, respectively (JCPDS File No. 28-0671). Here, it is worth pointing out that in the previous investigation [22] such major diffraction peaks were not observed even in a high  $\text{Nd}_2\text{O}_3$  loaded sample (36 wt%). Moreover, high loaded sample was annealed in air at comparatively high temperature ( $1000^\circ\text{C}$ ). It is expected that the absence of the strong diffraction peaks in the above study [22] is probably due to short sintering time. However, in our case, prolonged sintering at temperature of  $900^\circ\text{C}$  produces sharp diffraction peaks. We expect that during prolonged sintering, individual nanostructures merge together (process of particle fusion) and the activation energy becomes much larger and therefore

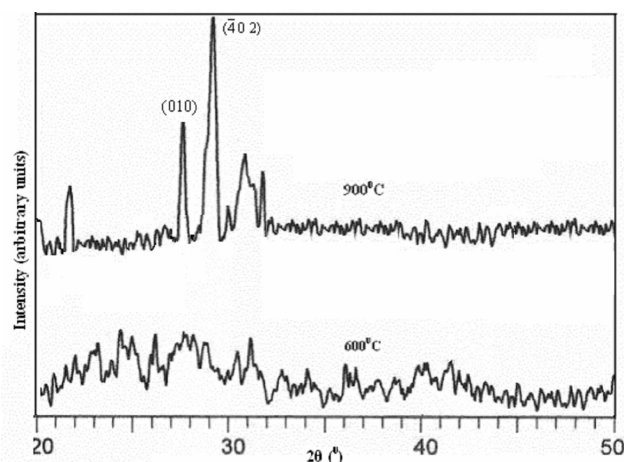


Fig. 1. XRD pattern of the  $\text{Nd}_2\text{O}_3$ -doped silica powder sample annealed at  $600^\circ\text{C}$  (6 h), and  $900^\circ\text{C}$  (12 h).

cross grain-boundary diffusion dominates over surface and volume diffusion process and eventually crystallinity increases. The sharp and strongest diffraction peak around  $2\theta \approx 29.2^\circ$  was employed to estimate the mean crystallite size of  $\text{Nd}_2\text{O}_3$  from the Scherrer formula and found to be  $\approx 12$  nm. The above results suggest that the thermal treatment of  $\text{Nd}_2\text{O}_3$ - $\text{SiO}_2$  composite system, synthesized by the solgel technique, at temperature of  $900^\circ\text{C}$  with prolonged sintering time (12 h) produces  $\text{Nd}_2\text{O}_3$ - $\text{SiO}_2$  nanocomposite system with distinct grain boundaries.

### 3.2. FTIR

FTIR transmittance spectra (range  $1250$ – $500$   $\text{cm}^{-1}$ ) of the heat-treated doped powdered samples are shown in Fig. 2. These spectra provide valuable information about the phase composition as well as bonding in the sintered composites. In FTIR spectrum of the sample sintered at  $600^\circ\text{C}$  for 6 h,  $800$ ,  $970$  and  $1090$   $\text{cm}^{-1}$  are the characteristics bands of amorphous  $\text{SiO}_2$ . The band at  $\approx 800$   $\text{cm}^{-1}$  may be assigned to vibration modes of ring structure of  $\text{SiO}_4$  tetrahedra [23]. The involvement of the polycondensation process is supported by the behavior of IR band at  $\approx 960$   $\text{cm}^{-1}$  associated with the stretching mode  $\text{Si-OH}$  of typical gel structure. The broad band  $\approx 1090$   $\text{cm}^{-1}$  is associated with the transversal optical (TO) mode of the  $\text{Si-O-Si}$  asymmetric stretching bond vibration. However, when the sample was sintered at  $900^\circ\text{C}$  for 12 h, many discrete bands appeared between  $640$  and  $970$   $\text{cm}^{-1}$ . In low frequency region of FTIR spectrum, the peak centered about  $650$   $\text{cm}^{-1}$  may be assigned to  $\text{Nd-OH}$  bond [16], while the weak peak at  $700$   $\text{cm}^{-1}$  is the metal-oxygen peak [24]. The characteristics band of neodymium silicates appeared around  $905$   $\text{cm}^{-1}$  and this band may be explained by the absorption due to asymmetric stretching mode vibration of  $\text{Si-O-Nd}$  bond. However, Ono and Katsumata [25] reported that asymmetric

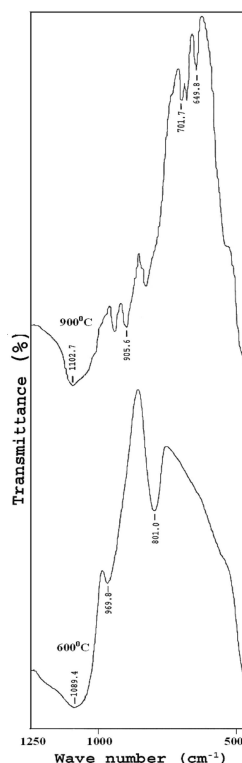


Fig. 2. FTIR spectra of  $\text{Nd}_2\text{O}_3$ -doped silica at different temperatures:  $600^\circ\text{C}$  (6 h), and  $900^\circ\text{C}$  (12 h).

stretching mode vibration of Si–O–Pr appears at  $900\text{ cm}^{-1}$ . In the present study the shift of the Si–O–Nd peak towards higher spatial frequency is a consequence of higher ionic radius of Nd than Pr. In addition, it was also observed that TO mode of the Si–O–Si slightly shifts towards a higher wave number with increasing sintering temperature and time. Similar behaviors of Si–O–Si band in annealed  $\text{SiO}_x$  ( $x$  — contents) sample were noticed by many workers [26–28]. They pointed out that the peak position of the asymmetric stretching broad band of the  $\text{SiO}_x$  sample depends on the oxygen contents. Nakamura et al. [26] and Milutinovic et al. [27] found that the oxygen contents decreases with increasing annealing temperature and time and as a result the peak position shifts towards higher wave number and eventually the density of  $\text{SiO}_x$  increases.

### 3.3. SEM

Figure 3 shows morphologies of the sintered composites systems ( $\text{Nd}_2\text{O}_3$ – $\text{SiO}_2$ ) as viewed under SEM. The SEM image (a) and (b) shows the morphology of agglomerated particles and quasi-spherical particles, respectively. Calcination of the sample at  $600^\circ\text{C}$  for 6 h may be contributed to agglomeration of the  $\text{Nd}_2\text{O}_3$  (in irregular shape) in silica matrix. It is expected that screening of uniform dis-

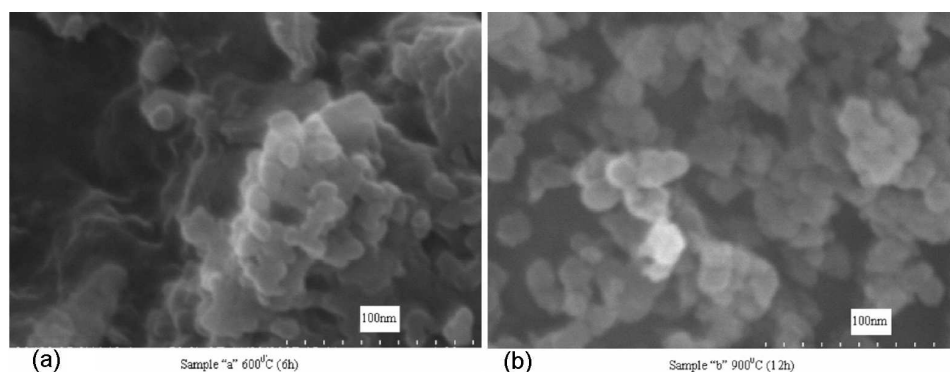


Fig. 3. SEM photograph of  $\text{Nd}_2\text{O}_3\text{-SiO}_2$  at (a)  $600^\circ\text{C}$  and (b)  $900^\circ\text{C}$ , respectively.

persion/distribution of  $\text{Nd}_2\text{O}_3$  in  $\text{SiO}_2$  matrix is due to concentration quenching. In order to overcome this problem, introduction and effect of the glass modifiers such as aluminum or phosphorous or suitable surfactants in  $\text{Nd}_2\text{O}_3\text{-SiO}_2$  binary system should be the subject of further investigation. Thermal treatment of the sample at comparatively high temperature ( $900^\circ\text{C}$ ) with prolonged sintering provides much-improved dispersion of  $\text{Nd}_2\text{O}_3$  in a fused silica matrix. Moreover, in this condition the shape of the particles is quasi-spherical with well defined grain boundaries. Here, it is worth pointing out that prolonged sintering favors the formation of a neodymium oxide with a fine substructure. This result also supports the observation made in X-ray diffraction. The above results infer that the microstructure of the  $\text{Nd}_2\text{O}_3\text{-SiO}_2$  composites obtained by solgel method can be controlled by selecting correctly both the heat treatment time and temperature.

#### 4. Conclusions

Using solgel method  $\text{Nd}_2\text{O}_3\text{-SiO}_2$  binary oxides (composites) with different structures were successfully obtained upon thermal treatment in air. During typical thermal treatment ( $900^\circ\text{C}/12\text{ h}$ ) the aggregation of powders is due to solid-state bonds formed between nanoparticles and fused silica matrix. The results suggest that sintering time and temperature plays pivotal role in the formation of monoclinic  $\text{Nd}_2\text{O}_3$  nanocrystallites as well as their distribution in fused silica matrix.

#### Acknowledgments

One of the authors (P.A) is thankful to Drs. K.C. Bhardwaj, P.K. Sen and N. Kishore for constant encouragement. Financial assistance from CSIR and DST (FIST) New Delhi India is gratefully acknowledged.

## References

- [1] R.W. Seigel, E. Hu, D.M. Cox, H. Goronkin, L. Jelinski, C.C. Kouch, M.C. Roco, D.T. Shaw, *WTEC Panel Report on Nanostructure Science and Technology*, International Technology Research Institute, 1998.
- [2] R.P. Andres, R.S. Averback, W.L. Brown, L.E. Brus, W.A. Goddard, A. Kaldor, S.G. Louie, M. Moscovits, P.S. Peercy, S.J. Riley, R.W. Siegel, F. Spaepen, Y. Wang, *J. Mater. Res.* **4**, 704 (1989).
- [3] S. Sun, C.B. Murray, *J. Appl. Phys.* **85**, 4325 (1999).
- [4] C. Suryanarayana, *Int. Mater. Rev.* **40**, 41 (1995).
- [5] F.E. Kruijs, H. Fissan, A. Peled, *J. Aerosol Sci.* **29**, 511 (1998).
- [6] G. Wakefield, H.A. Keron, P.J. Dobson, J.L. Hutchison, *J. Colloid Interface Sci.* **215**, 179 (1999).
- [7] W.X. Que, C.H. Kam, Y. Zhou, Y.L. Lam, Y.C. Chan, *J. Appl. Phys.* **90**, 4865 (2001).
- [8] R. Bazzi, M.A. Flores-Gonzales, C. Louis, K. Lebbou, C. Dujardin, A. Brenier, W. Zhang, O. Tillement, E. Bernstein, P. Perriat, *J. Lumin.* **102**, 445 (2003).
- [9] A.G. Dedov, A.S. Loktev, I.I. Moiseev, A. Aboukais, J.F. Lamonier, I.N. Filimonov, *Appl. Catal. A, Gen.* **245**, 209 (2003).
- [10] Y. Ozawa, Y. Tochihara, A. Watanabe, M. Nagai, S. Omi, *Chem. Lett.* **32**, 246 (2003).
- [11] S. Pengpanich, V. Meeyoo, T. Rirksomboon, *J. Chem. Eng. Jpn.* **38**, 49 (2005).
- [12] F.B. Noronha, D.A.G. Aranda, A.P. Ordine, M. Schmal, *Catal. Today* **57**, 275 (2000).
- [13] M. Zawadzki, L. Kepinski, *J. Alloys Comp.* **380**, 255 (2004).
- [14] S. Chevalier, G. Bonnet, J.P. Laprin, *Appl. Surf. Sci.* **167**, 125 (2000).
- [15] W. Que, X. Hu, L.H. Gan, G.R. Deen, *J. Mater. Res.* **17**, 1399 (2002).
- [16] L. Kepinski, M. Zawadzki, W. Mista, *Solid State Sci.* **6**, 1327 (2004).
- [17] R. Reisfeld, *J. Non-Crystal. Solids* **121**, 254 (1990).
- [18] E.J.A. Pope, J.D. Mackenzie, *J. Am. Ceram. Soc.* **76**, 1325 (1993).
- [19] M.J. Weber, *J. Non-Cryst. Solids* **123**, 208 (1990).
- [20] L.L. Hench, J.K. West, *Chem. Rev.* **90**, 33 (1990).
- [21] M. Zawadzki, L. Kepinski, *J. Alloys Comp.* **380**, 255 (2004).
- [22] L. Kepinski, M. Wolcyrz, M. Drozd, *Mater. Chem. Phys.* **96**, 353 (2006).
- [23] M. Decottignies, J. Phalippou, J. Zarzycki, *J. Mater. Sci.* **13**, 2605 (1978).
- [24] B. Zhaorigetu, G. Ridi, L. Min, *J. Alloys Comp.* **427**, 235 (2007).
- [25] H. Ono, T. Katsumata, *Appl. Phys. Lett.* **78**, 1832 (2001).
- [26] M. Nakamura, Y. Mochizuki, K. Usami, Y. Itoh, T. Nozaki, *Solid State Commun.* **50**, 1079 (1984).
- [27] A. Milutinovic, Z. Dohcevic-Mitrovic, D. Nesheva, M. Scepanovic, M. Grujic-Brojcin, Z.V. Popovic, *Mater. Sci. Forum* **555**, 309 (2007).
- [28] D.V. Tsu, G. Lucovsky, B.N. Davidson, *Phys. Rev. B* **40**, 1795 (1989).